Applied Physics A (2022) 128:775
https://doi.org/10.1007/s00339-022-05914-1

Applied Physics A
Materials Science & Processing

S.I. : COLA 2021/2022

Luminescent carbon nanostructures synthesized by ultrasound-assisted laser ablation in liquid media

L. Escobar-Alarcon[1] · A. Limas-Escobar[2] · D. A. Solis-Casados[3] · S. Romero[1] · E. Haro-Poniatowski[2]

Received: 24 May 2022 / Accepted: 30 July 2022

Abstract

In this work, it is shown that the use of liquid laser ablation assisted by an ultrasonic field allows the preparation of carbon nanostructures with photoluminescent properties. The ablation of a high purity carbon target submerged in deionized water, in absence and in presence of an ultrasonic field, variable in power and frequency, was performed using a nanosecond Nd:YAG laser emitting at 1064 nm. The obtained nanostructures were characterized by UV–Vis, Raman, and Photoluminescence spectroscopies, as well as by Scanning and Transmission Electron Microscopies. In general terms, the characterization results reveal important effects due to the application of the ultrasonic field, particularly, modifying their photoluminescence emission properties.

Keywords Carbon nanostructures · Photoluminescence · Laser ablation in liquid media

1 Introduction

Laser ablation in liquids has been widely used to produce a variety of nanostructures with different shapes and sizes of metals, alloys, and oxides, with applications in different scientific and technological areas [1–7]. An important advantage of this method is its versatility enabling its combination with other techniques in an easy way. The combination of laser ablation in liquids with an ultrasound field has already been investigated to study the effects of the ultrasonic excitation on the structure of laser-ablated nanoparticles and it has been found to lead to an enhancement of the production rate of the nanoparticles [8]. In previous works, we have reported that the combination of ultrasound with laser ablation results in important changes in the morphology of the nanostructures producing nanosheets in colloidal suspensions [9, 10]. In addition, we have shown that the combination of laser ablation in liquid media of some metals with an ultrasonic field allows the generation of hydrogen directly by water splitting. The proposed procedure has as main advantages the generation of H_2 of high purity as well as a low amount of metal mass consumed leading to maximum production rates close to 1300 mL/min/gr of aluminum, comparable or even higher than previously reported values. At the same time, nanomaterials in colloidal form are produced; this proposed procedure is then a bifunctional method [11, 12].

Concerning carbon nanostructures, it has been observed that they exhibit interesting properties; particularly, fluorescence of carbon nanoparticles has attracted increasing research attention due to their promising applications ranging from electro-optics to bio-nanotechnology [13]; currently photoluminescent nanoparticles have been developed from lead, cadmium and silicon compounds, but it has been observed that these materials are the cause of some health problems due to their potential toxicity, environmental damage and poor photostability [10, 13]. Fluorescent carbon nanostructures are stable and less toxic being suitable for biological applications [13]. In this work, it is shown that the use of liquid laser ablation assisted by an ultrasonic field allows the preparation of carbon nanostructures with photoluminescent properties.

✉ E. Haro-Poniatowski
haro@xanum.uam.mx

[1] Departamento de Física, Instituto Nacional de Investigaciones Nucleares, Carr. México-Toluca S/N, La Marquesa Ocoyoacac, C.P. 52750 Estado de México, México

[2] Departamento de Física, Universidad Autónoma Metropolitana Iztapalapa, Apdo. Postal 55-534 Mexico City, México

[3] Universidad Autónoma del Estado de México. Centro Conjunto de Investigación en Química Sustentable UAEM-UNAM, C.P. 50200 Estado de México, México

2 Experimental procedure

The carbon nanostructures were prepared by laser ablation in liquid media without and with the assistance of different ultrasonic fields. A high purity (99.99%) graphite disk target, with a diameter of 2.5 cm and thickness of 0.6 cm, was submerged in 10 mL of distilled water. Laser ablation was carried out using a Nd:YAG laser at wavelength of 1064 nm and 5 ns of pulse duration, with a repetition rate of 10 Hz. First, experiments at three different laser fluences, 3.0, 4.5 and 7.2 J/cm^2 were performed. The ablation time was kept constant at 15 min for all samples. For the experiments with ultrasonic excitation, an ultrasonic bath with variable power, from 30 to 100 W, and two frequencies, 37 and 80 kHz, was used. The laser beam was focused onto the target surface using a quartz lens with 12 mm of focal length. Figure 1 shows a schematic of the experimental setup combining laser ablation with an ultrasonic field. The obtained carbon nanostructures were characterized by Scanning Electron Microscopy (SEM, JSM6610-LV), Transmission Electron Microscopy (TEM, JEOL 2100), and Raman spectroscopy (HR LabRam 800 system). For the TEM characterization, a drop of each of the prepared colloids was deposited on TEM 300 mesh copper grids with a carbon layer. The same was done on pieces of silicon wafers for SEM and Raman spectroscopy measurements. Optical absorption (Perkin Elmer lambda-35 spectrometer) and Photoluminescence (FluoroMax 4, Horiba Jobin Yvon) measurements were performed using directly the prepared colloids containing carbon nanostructures.

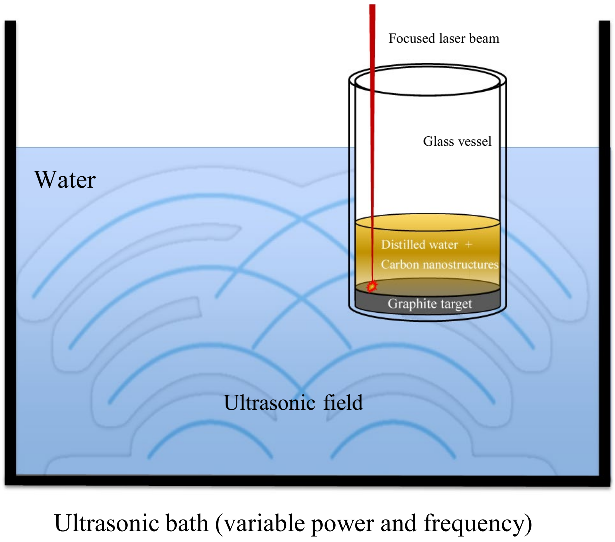

Fig. 1 Schematic of the experimental setup combining laser ablation with an ultrasonic field of variable power and frequency

3 Results

3.1 Scanning electron microscopy characterization

Figure 2a–d shows SEM images of samples prepared under different experimental conditions with and without the presence of the ultrasonic field. The image of the sample made without ultrasound assistance at a laser fluence of 4.5 J/cm^2 is shown in Fig. 2a. Laminar nanostructures with sizes of approximately 1 µm with regular shapes and little agglomeration are obtained; in addition, some two-dimensional nanostructures of lower size are present. In Fig. 2b nanostructures prepared in the presence of an ultrasonic field at a frequency of 37 kHz and a power of 30 W are observed. In this case, more agglomerated laminar structures of approximately 5 µm of size and in some cases irregular shapes are present. When an ultrasonic field of 80 kHz and 100 W is applied, the nanostructures reduce their size, increasing their stacking and an increase in the number of smaller nanostructures is observed as shown in Fig. 2c. Finally, if a field of 37 kHz and 100 W is used the laminar structures disappear, instead agglomerated particles of smaller sizes with a large number of stacked sheets are formed as it is shown in Fig. 2d.

3.2 Transmission electron microscopy characterization

Figure 3 shows TEM images of the samples produced with and without ultrasonic excitation. In general terms, all samples show the presence of 2D nanostructures and particles with different sizes and irregular shapes, the presence of sheets with less stacking are observed in presence of ultrasonic excitation (Fig. 3c, d). Figure 3a shows the nanostructures obtained without ultrasound at a laser fluence of 4.5 J/cm^2; agglomerated carbon quasispheroidal nanoparticles with sizes ranging from 10 to 20 nm and some nanosheets are observed. In the case of samples prepared in the presence of an ultrasonic field of 37 kHz and 100 W (Fig. 3b) the spheroidal nanoparticles appear as well but in a lower quantity, whereas more regular two-dimensional structures with a high degree of agglomeration are present. At a frequency of 37 kHz and a power of 30 W of the applied ultrasound field the production of laminar nanostructures is promoted as seen in Fig. 3c. It is worth noting the presence of carbon single-layers in this image in which some carbon sheets reach sizes of hundreds of nm with very regular shapes. As in a previous work [10], these results suggest that the presence of the ultrasonic field during laser ablation in liquid favors the formation of graphene nanosheets composed from 1

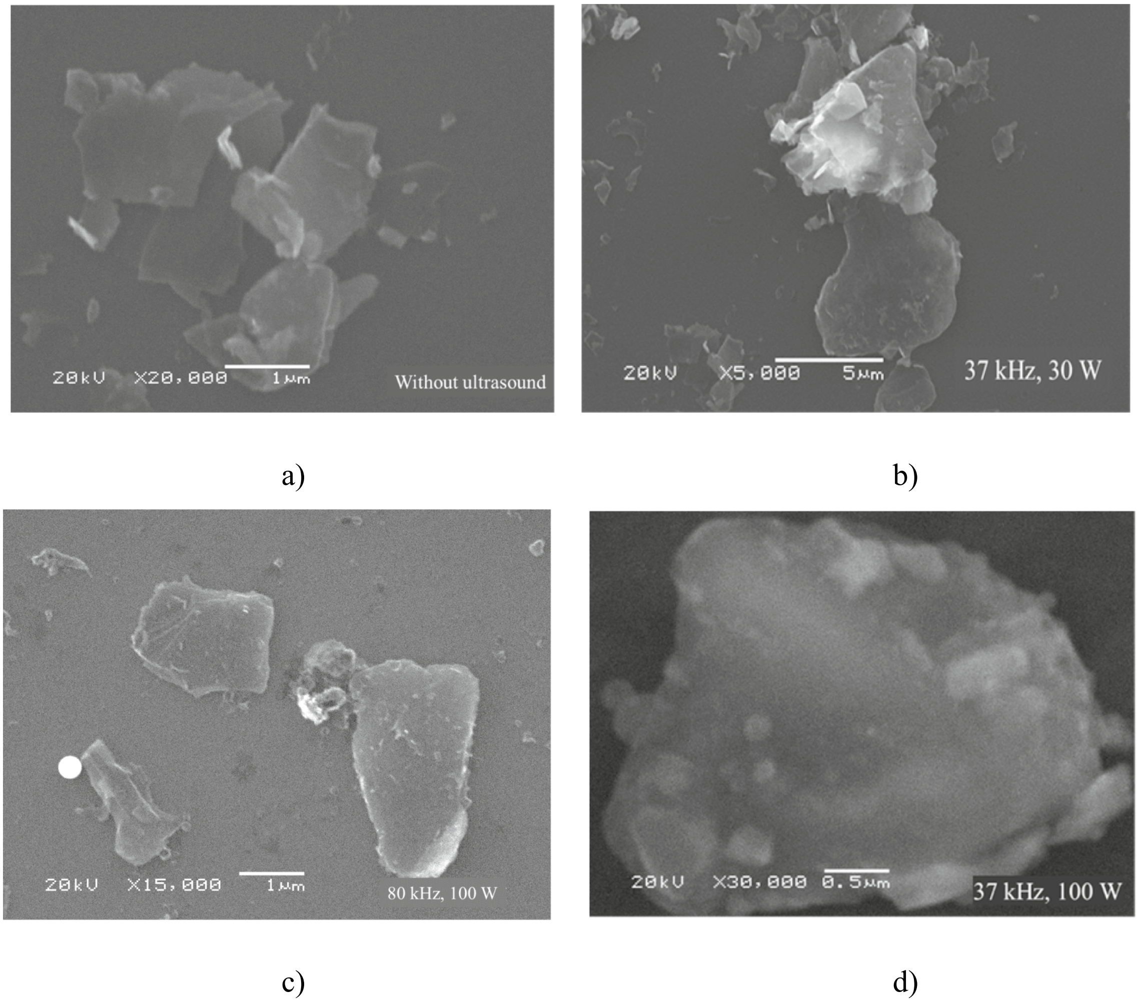

a)

b)

c)

d)

Fig. 2 SEM images of the different carbon nanostructures prepared, **a** without ultrasound assistance, **b** With ultrasonic field: 30 W, 37 kHz, **c** With ultrasonic field: 100 W, 80 kHz, **d** With ultrasonic field: 100 W, 37 kHz,

to a few layers only. Finally, the samples prepared in the presence of an ultrasonic field at a frequency of 80 kHz and a power of 100 W show laminar nanostructures with a less regular shape and nanoparticles with sizes of around 20 nm, in addition another type of carbon nanostructures similar to carbon nanofoam reported in [14] are observed.

3.3 Raman spectroscopy characterization

The structural characterization of the prepared carbon nanostructures was performed using Raman spectroscopy, this technique can differentiate the various forms of carbon-based materials [15, 16]. Figure 4a shows the Raman spectra of the samples obtained at different laser fluences. These spectra show the D, G and 2D bands characteristic of this type of materials. Although in general terms the spectra are very similar some differences are evident, for example, the intensity and shape of the 2D band is different in each case; furthermore, the shape of the G band and the ratio of intensities of the G to D bands is also different. A clear difference observed for the sample prepared at a fluence of 4.5 J/cm^2 is its higher ratio of the 2D/G peak intensities suggesting a higher graphene content. Figure 4b shows the Raman spectra of samples prepared at the same laser fluence (4.5 J/cm^2) with and without ultrasonic excitation. To compare clearly the differences between the Raman spectra of these samples, these were scaled to have similar intensity of the G peak. Several features are clearly observed. An evident lower intensity of the D band in the sample prepared using an ultrasonic field at a frequency of 37 kHz and a power of 30 W is seen. It is well known that this band arises due to the presence of defects or disorder [17] indicating a higher degree of order in this sample. This is consistent with the transmission electron microscopy results (Fig. 3a), since samples prepared in these conditions are formed by nanosheets with very regular shapes and low agglomeration.

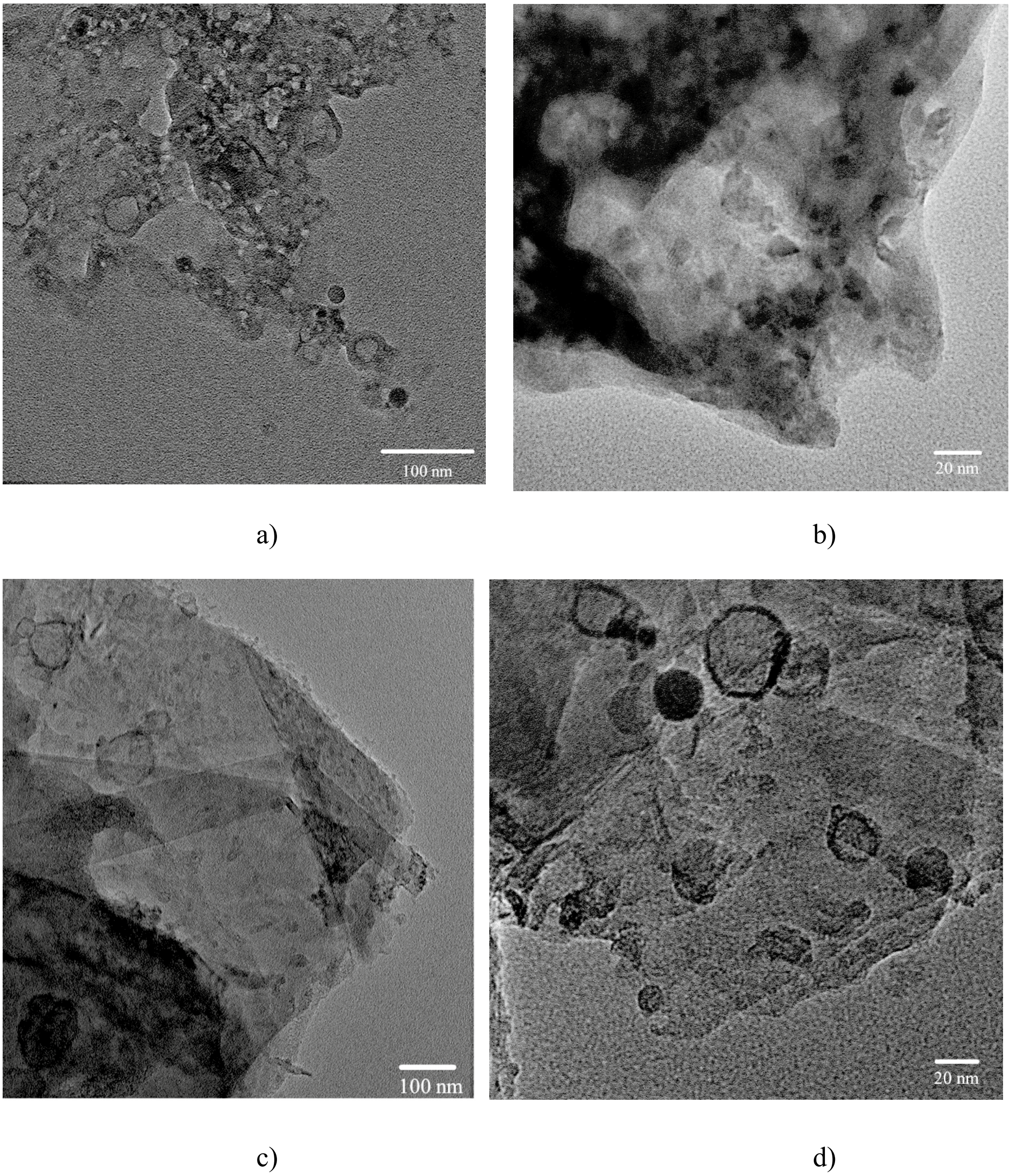

a)

b)

c)

d)

Fig. 3 TEM images of the different carbon nanostructures prepared, **a** without ultrasound assistance, **b** With ultrasonic field: 30 W, 37 kHz, **c** With ultrasonic field: 100 W, 80 kHz, **d** With ultrasonic field: 100 W, 37 kHz,

In addition, clear differences are observed in the intensity and shape of the 2D band suggesting changes in the microstructure due to the presence of the ultrasonic field. The spectrum of the sample prepared using an ultrasonic field at a frequency of 37 kHz and a power of 100 W reveals a very wide G band indicative of a highly disordered material which can be attributed to the fact that at the highest power of the ultrasonic field delamination of the carbon agglomerates is produced as well as their disordering.

3.4 UV–Vis spectroscopy characterization

The optical absorption spectra of the samples prepared at different laser fluences without the ultrasonic field are shown in Fig. 5a. These spectra show the peak of absorption characteristic of nanostructured carbon, around 265 nm, attributed to transitions π–π^* of C–C bonds, in good agreement with previous reports [18, 19]. It is worth mentioning that CnH_2 polyynes formed by laser ablation of graphite

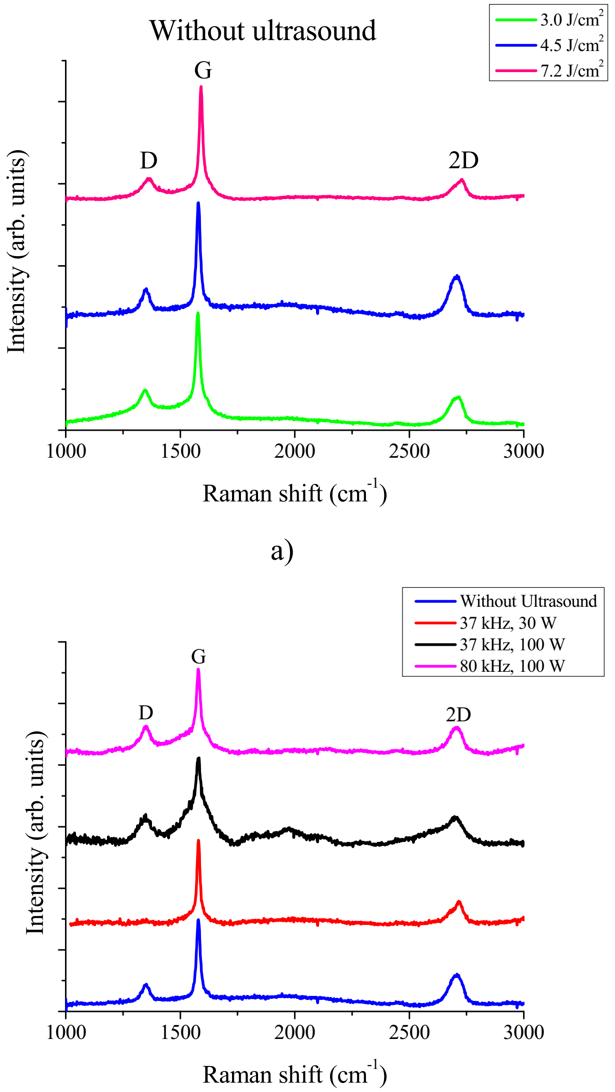

a)

b)

Fig. 4 **a** Raman spectra of carbon nanostructures obtained at different laser fluences without ultrasonic field, **b** Raman spectra of carbon nanostructures prepared in presence of the ultrasonic field in different conditions

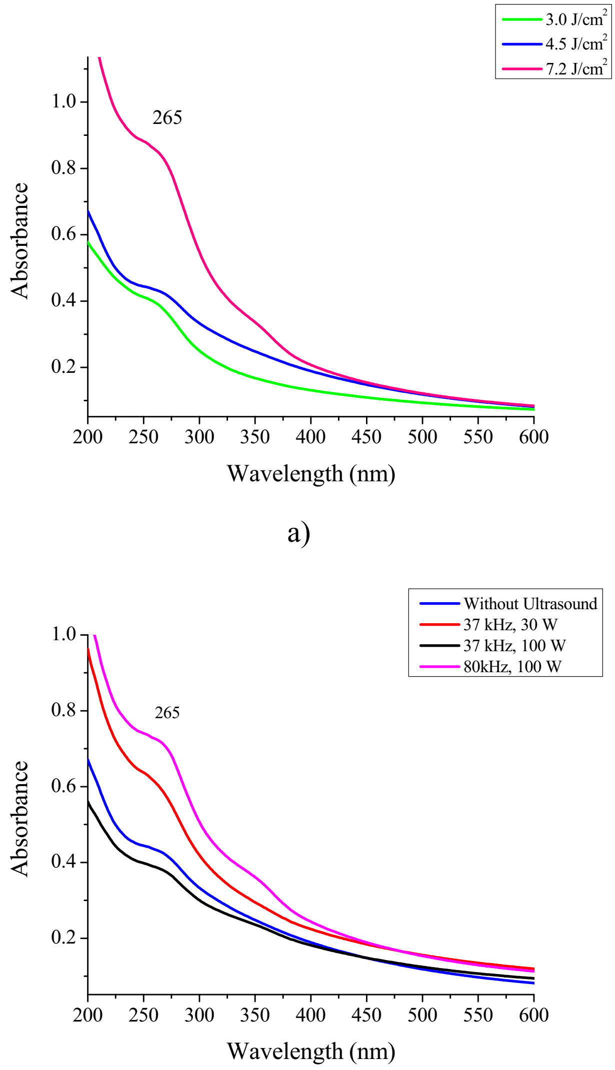

a)

b)

Fig. 5 **a** Absorbance of carbon nanostructures obtained at different laser fluences without ultrasonic field, **b** Absorbance of carbon nanostructures prepared in presence of the ultrasonic field in different conditions

and C60 particles suspended in benzene, toluene, or hexane solution are characterized by absorption bands below 330 nm depending on the linear polyyne structure [20, 21]. Particularly, the $C_{12}H_2$ shows absorbance bands at 236, 247 and 273 nm, [20]. These bands lie close to the maximum observed in the spectra of Fig. 5. However, it has been reported that the hydrogen concentration in the solvent plays an important role in the formation of polyynes and in their abundance, which is higher at higher H concentrations [21]. In this case, H_2O was used with a very low amount of H compared for example with hexane (C_6H_{14}) in which a very low contribution of polyynes to the absorbance spectra in Fig. 5 is expected. It is observed that as the laser fluence increases, the absorbance increases indicating a higher production of carbon nanostructures. In the case of the colloids obtained under the same experimental conditions, but in the presence of the ultrasonic field (Fig. 5b), the characteristic peak around 265 nm is still observed, although it is evident that there is an important effect due to ultrasound; first, it is observed that the samples prepared with ultrasonic excitation have a higher absorbance than the sample prepared without ultrasound, reaching practically two times the absorbance, indicative of a bigger amount of carbon nanostructures suggesting that ultrasound favors a more efficient production. Concerning the effect of the ultrasonic field, it is observed that for the same frequency (37 kHz) the sample prepared at an ultrasound power of 30 W increases its absorbance by 47%, while at a power of 100 W a decrease in absorbance of approximately 7% is detected. The effect of the frequency of the ultrasonic field keeping the power at 100 W, reveals that at 80 kHz the maximum absorbance is reached, approximately 80% higher than for the sample prepared without ultrasound.

3.5 Photoluminescence characterization

Figure 6 shows the photoluminescence spectra corresponding to the samples prepared at different laser fluence without the presence of the ultrasonic field obtained using an excitation wavelength at 290 nm. A photoluminescent blue emission varying from 438 to 421 nm is observed. When the laser fluence increases, the intensity of the emission increases and shifts to lower wavelengths. This result suggests that an increase in the laser fluence produces smaller nanostructures, since smaller sizes increase the effects of quantum confinement producing emission at higher energies [22]. Figure 6b shows that the emission shifts to shorter wavelengths following an approximately linear monotonous behavior. Figure 7 shows the behavior of the luminescent emission as a function of the excitation wavelength for the sample prepared at a laser fluence of 4.5 J/cm^2 in absence of the ultrasonic field. It is observed that when the excitation wavelength increases, the emission shifts to longer wavelengths following an approximately linear monotonous behavior as is shown in Fig. 7b. This result suggests that the PL emission can be tuned by changing the excitation

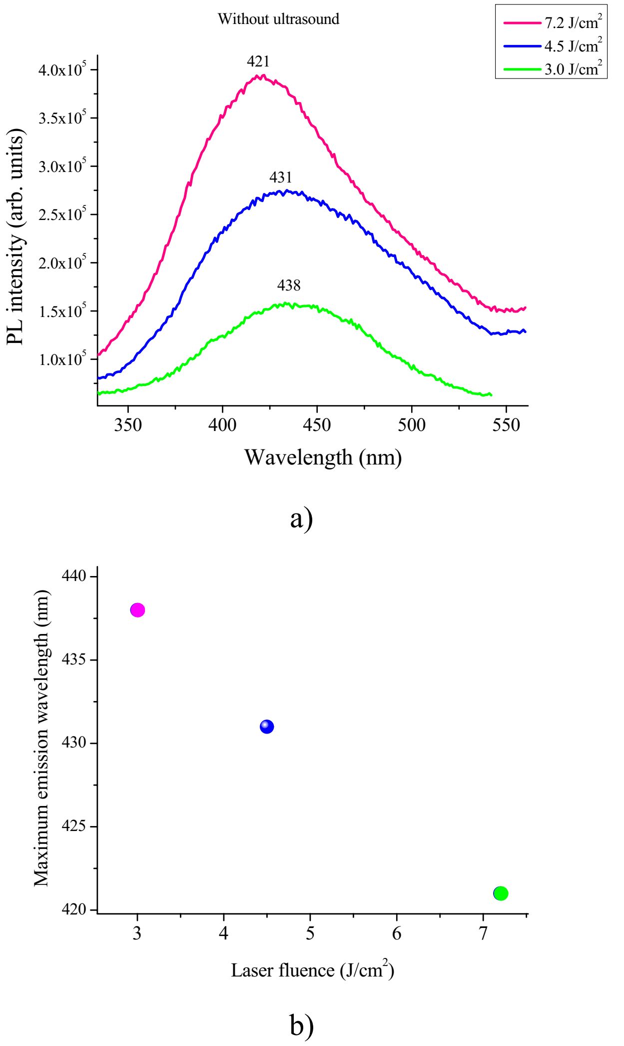

a)

b)

Fig. 6 **a** PL emission of carbon nanostructures obtained at different laser fluences without ultrasonic field, **b** maximum emission wavelength as a function of the laser fluence

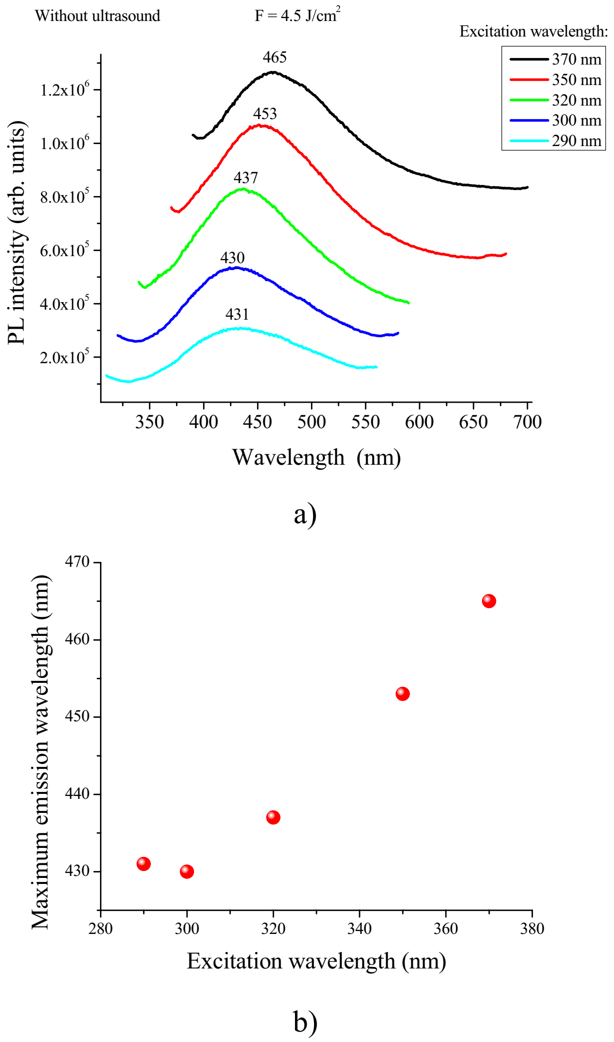

a)

b)

Fig. 7 **a** PL emission of carbon nanostructures obtained at 4.5 J/cm^2 without ultrasonic field as a function of the excitation wavelength, **b** Maximum emission wavelength as a function of the excitation wavelength

wavelength. Figure 8a presents the behavior of the photoluminescent emission as a function of the excitation wavelength for the sample prepared at a laser fluence of 4.5 J/cm^2 in the presence of an ultrasonic field of 30 W of power and a frequency of 37 kHz. It is evident that the presence of the ultrasonic field significantly modifies the photoluminescent emission, in this case, a shift to shorter wavelengths is observed when the excitation wavelength increases, behavior contrary to the observed [23] which could be attributed to the different kind of formed nanostructures with smaller sizes. At the higher excitation wavelength, higher than 320 nm, a shift to longer wavelengths is observed.

The photoluminescent emission as a function of the excitation wavelength for the sample prepared at a laser fluence of 4.5 J/cm^2 in the presence of an ultrasonic field of 100 W of power and a frequency of 80 kHz is shown in Fig. 9a. In this case, a blue shift for wavelengths lower than 320 nm is observed. On the contrary, excitation at a longer wavelength produces the opposite effect as it is observed in Fig. 9b. The blue shift for ultrasound-prepared samples is consistent with a decrease in the size of the quantum carbon dots present in these samples. However, the origin of this behavior is unclear, it can be speculated that the presence of size and shape effects of nanostructures prepared under the presence of an ultrasonic field significantly affect the luminescent properties of the carbon nanostructures.

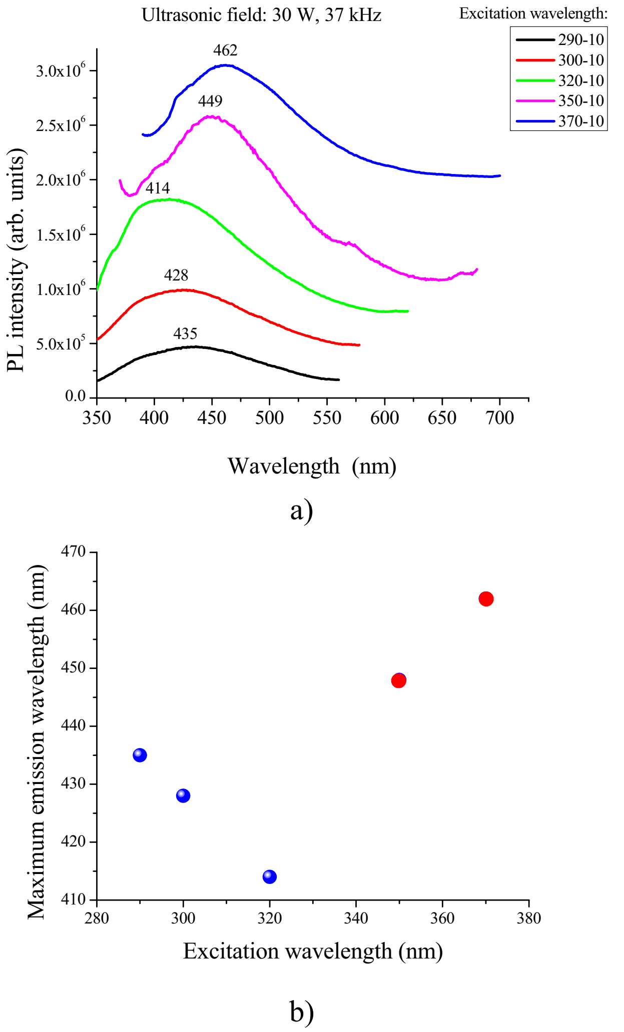

a)

b)

Fig. 8 **a** PL emission of carbon nanostructures obtained at 4.5 J/cm^2 with ultrasonic field: 30 W and 37 kHz, as a function of the excitation wavelength, **b** maximum emission wavelength as a function of the excitation wavelength

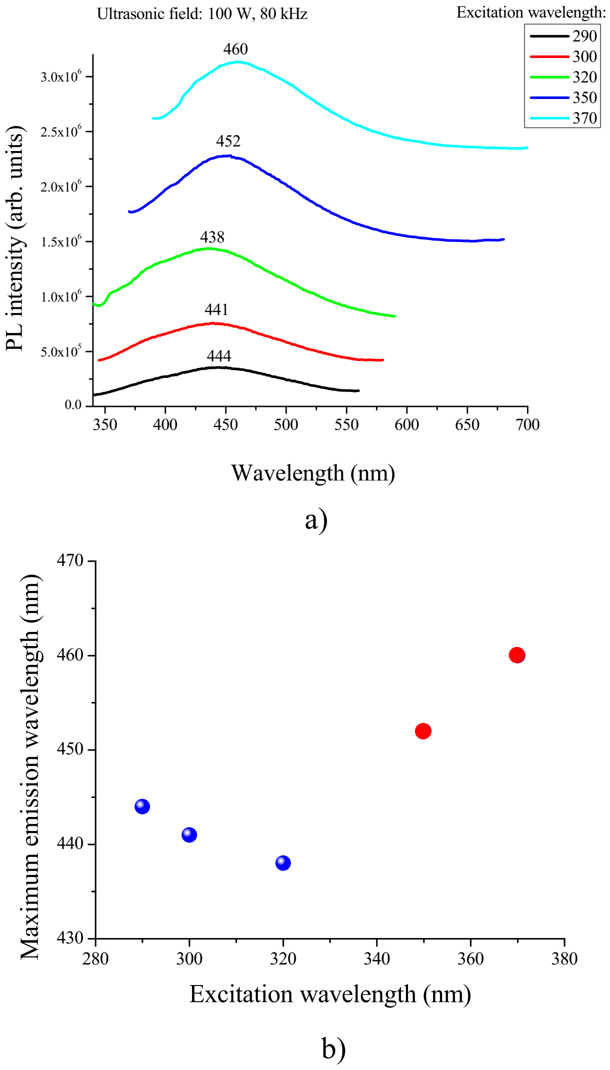

a)

b)

Fig. 9 PL emission of carbon nanostructures obtained at 4.5 J/cm^2 with ultrasonic field: 100 W and 80 kHz, as a function of the excitation wavelength, **b** maximum emission wavelength as a function of the excitation wavelength

4 Conclusions

Carbon nanostructures were successfully synthesized by laser ablation in distilled water without and in presence of ultrasonic fields under different power and frequency conditions. The results of the characterization techniques showed that the ultrasonic field has important effects on the size and shape of the carbon nanostructures obtained. The photoluminescence characterization showed a blue emission that can be changed in the range of 410–470 nm depending on the excitation wavelength in the UV region of the spectrum.

Acknowledgements The ININ support through the project CB-004 is acknowledged. The technical support with TEM and SEM measurements provided by I. Martinez Mera and J. Perez del Prado, respectively, is also recognized.

Declarations

Conflict of interest The authors declare that they have no conflict of interest.

References

1. S.I. Dolgaev, A.V. Simakin, V.V. Voronov, G.A. Shafeev, F. Bozon-Verduraz, Appl. Surf. Sci. **186**, 546 (2002)
2. V. Amendola, S. Scaramuzza, F. Carraro, E. Cattaruzza, J. Colloid Interface Sci. **489**, 18 (2017)
3. A. Singh, J. Vihinen, E. Frankberg, L. Hyvärinen, Mari honkanen and erkki levänen. Nanoscale Res. Lett. **11**, 447 (2016)
4. V. Amendola, M. Meneghetti, Phys. Chem. Chem. Phys. **15**, 3027 (2013)
5. E. Fazio, B. Gökce, A. De Giacomo, M. Meneghetti, G. Compagnini, M. Tommasini, F. Waag, A. Lucotti, C.G. Zanchi, P.M. Ossi, M. Dell'Aglio, L. D'Urso, M. Condorelli, V. Scardaci, F. Biscaglia, L. Litti, M. Gobbo, G. Gallo, M. Santoro, S. Trusso, F. Neri, Nanomaterials **10**(11), 2317 (2020)
6. H. Zeng, Du. Xi-Wen, S.C. Singh, S.A. Kulinich, S. Yang, J. He, W. Cai, Adv. Funct. Mater. **22**, 1333 (2012)
7. D. Zhang, B. Gökce, S. Barcikowski, Chem. Rev. **117**(5), 3990 (2017)
8. S. Dadras, P. Jafarkhanu, M.J. Torkamany, J. Sabbaghzadeh, J. Phys. D. Appl. Phys. **42**, 025405 (2009)
9. L. Escobar-Alarcón, E. Velarde-Granados, D.A. Solís-Casados, O. Olea-Mejía, M. Espinosa-Pesqueira, E. Haro-Poniatowski, Appl. Phys. A. (2016). https://doi.org/10.1007/s00339-016-9992-z
10. L. Escobar-Alarcón, M.E. Espinosa-Pesqueira, D.A. Solis-Casados, J. Gonzalo, J. Solis, M. Martinez-Orts, E. Haro-Poniatowski, Appl. Phys. A **124**, 141 (2018)
11. L. Escobar Alarcón, J.L. Iturbe-García, F. González-Zavala, D.A. Solis-Casados, R. Pérez-Hernández, E. Haro-Poniatowski, Appl. Surface Sci **478**, 189–196 (2019)
12. L. Escobar Alarcón, J.L. Iturbe-García, F. González-Zavala, D.A. Solis-Casados, R. Pérez-Hernández, E. Haro-Poniatowski, Int. J. Hydro. Energy. **44**(3), 1579–1585 (2019)
13. H. Li, X. He, Y. Liu, H. Huang, S. Lian, S.-T. Lee, Z. Kang, Carbon **49**, 605 (2011)
14. J.L. Elechiguerra, J.L. Burt, J.R. Morones, A. Camacho-Bragado, X. Gao, H.H. Lara, M.J. Yacaman, J. Nanobiotechnol. **3**, 6 (2005)
15. A.C. Ferrari, J.C. Meyer, V. Scardaci, C. Casiraghi, M. Lazzeri, F. Mauri, S. Piscanec, D. Jiang, K.S. Novoselov, S. Roth, A.K. Geim, Phys. Rev. Lett. **97**, 187401 (2006)
16. A.C. Ferrari, D.M. Basko, Nat. Nanotechnol. **8**, 235 (2013)
17. A.C. Ferrari, Solid State Commun. **143**, 47 (2007)
18. S. Zhu, Y. Song, J. Wang, H. Wan, Y. Zhang, Y. Ning, B. Yang, Nano Today **13**, 10 (2017)
19. N. Takada, A. Fujikawa, N. Koshizaki, K. Sasaki, Appl. Phys. A **110**, 885 (2013)
20. M. Tsuji, T. Tsuji, S. Kuboyama, S.-H. Yoon, Y. Korai, T. Tsujimoto, K. Kubo, A. Mori, I. Mochida, Chem. Phys. Lett. **355**, 101 (2002)
21. M. Tsujia, S. Kuboyama, T. Matsuzaki, T. Tsuji, Carbon **41**, 2141 (2003)
22. S.K. Mahasin Alam, A. Ananthanarayanan, L. Huang, K.H. Lim, P. Chen, J. Mater. Chem. C. **2**, 6954 (2014)
23. V. Singh, K.S. Rawat, S. Mishra, T. Baghel, S. Fatima, A.A. John, N. Kalleti, D. Singh, A. Nazir, S.K. Rath, A. Goel, J. Mater. Chem. B **6**, 3366 (2018)